JACS
JOURNAL OF THE AMERICAN CHEMICAL SOCIETY
Communication
pubs.acs.org/JACS

Yolk/Shell Assembly of Gold Nanoparticles by Size Segregation in Solution

Jinjian Wei,[†,¶] Kenichi Niikura,[*,‡,¶] Takeshi Higuchi,[§] Takashi Kimura,[‡] Hideyuki Mitomo,[‡] Hiroshi Jinnai,[*,§] Yasumasa Joti,[⊥] Yoshitaka Bessho,[∥,#] Yoshinori Nishino,[*,‡] Yasutaka Matsuo,[‡] and Kuniharu Ijiro[‡]

[†]Graduate School of Chemical Science and Engineering, Hokkaido University, Sapporo 060-8628, Japan
[‡]Research Institute for Electronic Science, Hokkaido University, Sapporo 001-0021, Japan
[§]Institute of Multidisciplinary Research for Advanced Materials, Tohoku University, Sendai, Miyagi 980-8577, Japan
[⊥]Japan Synchrotron Radiation Research Institute/SPring-8, 1-1-1 Kouto, Sayo-cho, Sayo-gun, Hyogo 679-5198, Japan
[∥]RIKEN SPring-8 Center, 1-1-1 Kouto, Sayo-cho, Sayo-gun, Hyogo 679-5148, Japan
[#]Institute of Physics, Academia Sinica, 128 Sec. 2, Academia Rd., Nankang, Taipei 11529, Taiwan

Supporting Information

ABSTRACT: We demonstrate that binary mixtures of small and large gold nanoparticles (GNPs) (5/15, 5/30, 10/30, and 15/30 nm in diameter) in the presence of a glucose-terminated fluorinated oligo(ethylene glycol) ligand can spontaneously form size-segregated assemblies. The outermost layer of the assembly is composed of a single layer of small-sized GNPs, while the larger-sized GNPs are located in the interior, forming what is referred to as a yolk/shell assembly. Time course study reveals that small and large GNPs aggregate together, and these kinetically trapped aggregations were transformed into a size-segregated structure by repeating fusions. A yolk/shell structure was directly visualized in solution by X-ray laser diffraction imaging, indicating that the structure was truly formed in solution, but not through a drying process.

The controllable self-assembly of metal nanoparticles (NPs) has attracted a good deal of attention recently due to their wide-ranging potential applications.[1−5] Various soft bottom-up approaches based on NP functionalization for their self-assembly have been explored,[6−16] such as single-chain ligand coating,[6] DNA hybridization,[7−9] liquid crystal functionalization,[10−12] and dendronization of NPs.[13−16] To achieve NP assemblies applicable to increasingly complex and novel functionalities, the self-assembly of NPs of different compositions or sizes is practically attractive. The assembly of NPs of different composites or sizes into a binary NP superlattice with a crystalline structure has been widely explored.[17−20] Theoretical and experimental studies on the phase segregation of NPs of different sizes and shapes have been reported.[21−23] However, the segregation in these studies was achieved on a solid substrate or liquid/air interface with external forces, such as a solvent evaporation or capillary force.[24−26] Kiely et al. found that alkanethiol-coated gold nanoparticles (GNPs) of different sizes could spontaneously organize themselves into size-segregated regions during the drying process.[24] The size ratio of NPs is generally considered to be important for the size segregation process, which is believed to result mainly from entropy maximization.[27−29] In addition, vertical segregation has been achieved by the self-assembly of binary mixtures of NPs at a liquid/air interface.[25] Solution-based hierarchical assembly, which could simplify and extend the potential applications of functional NPs, still remains as an important theme.

Recently, we developed a nontemplate approach to the fabrication of gold nanoparticle vesicles (GNVs) through the self-assembly of semifluorinated oligo(ethylene glycol) (OEG)-tethered GNPs.[30] However, little is known about the hierarchical assembly of binary mixtures of NPs even though vesicular assembly of NPs made of single kind and size of NPs have been explored.[31,32] Herein, we present a rational design using a glucose-terminated fluorinated OEG ligand (GFL) as the carbohydrate can provide inter- and intramolecular hydrogen bonding,[33,34] thus providing stronger interactions than OEG. In this Communication, we report that binary mixtures of small and large GNPs modified with GFL spontaneously self-assemble into a size-segregated yolk/shell structure in solution, in which clusters of large GNPs are covered with a monolayer of small GNPs due to entropy-driven size segregation (Scheme 1).

First, we tested GNVs formation using newly synthesized ligand GFL. Citric acid-coated GNPs with a diameter of 15 nm (referred to as Au-15, 50 μL of H_2O) were added to GFL dissolved in dioxane (450 μL). Spherical assemblies (Figure S1a) with a hydrodynamic diameter of ∼120 nm, as measured by dynamic light scattering (DLS) (Figure S2), were formed in dioxane. Transmission electron microscopy (TEM) images (Figures 1a and S1b) show an obvious contrast between the edge and the center of the assemblies, indicating a hollow structure. Transmission electron microtomography (TEMT) was further carried out to confirm the inside of the assemblies. The reconstructed images (Figure 1b and Supporting Movie 1) clearly demonstrate a spherical hollow structure with a monolayer of GNPs.

Received: November 29, 2015
Published: February 29, 2016

DOI: 10.1021/jacs.5b12456
J. Am. Chem. Soc. 2016, 138, 3274−3277

Scheme 1. Chemical Structure of GFL Used in This Study, and Self-Assembly of the Binary Mixtures of GNPs with GFL into a Yolk/Shell Assembly

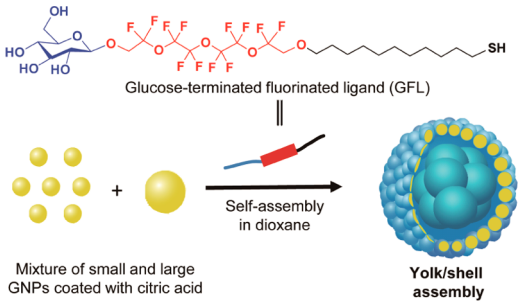

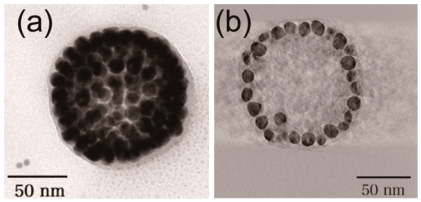

Figure 1. (a) TEM image of a Au-15 NP assembly. (b) XY image digitally sliced approximately in the middle of the Au-15 NP assembly; data from a reconstructed TEMT 3D image of (a). Note that the electrons were irradiated along the Z direction (perpendicular to the image (b) in TEM). This indicates that the addition of GFL to small GNPs (15 nm) produces GNVs.

We next examined vesicle formation using Au-15 NPs in the presence of Au-30 NPs. Mixtures of Au-30 and Au-15 NPs (the number ratio: $N_{Au\text{-}15}$:$N_{Au\text{-}30}$ = 7:1, 50 μL) with GFL in dioxane (450 μL) produced spontaneous self-assembly into a size-segregated structure (Figures 2a and S3). The surface of NP

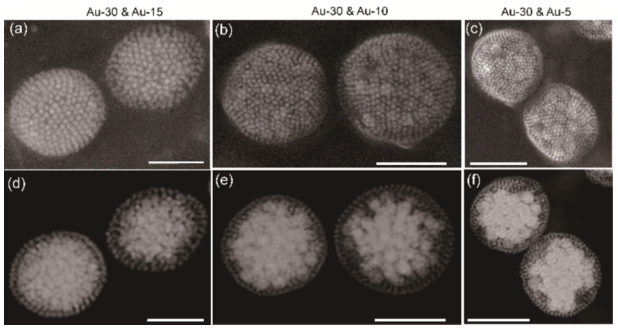

Figure 2. (a–c) SE-SEM and (d–f) HAADF-STEM images of small and large NPs mixtures with GFL: (a,d) Au-30 and Au-15 ($N_{Au\text{-}15}$:$N_{Au\text{-}30}$ = 7:1), (b,e) Au-30 and Au-10 ($N_{Au\text{-}10}$:$N_{Au\text{-}30}$ = 10:1), and (c,f) Au-30 and Au-5 ($N_{Au\text{-}5}$:$N_{Au\text{-}30}$ = 100:1) NPs. All scale bars are 150 nm.

assemblies was imaged based on the secondary electron mode of scanning transmission electron microscopy (SE-SEM). The interior of NP assemblies was acquired using high-angle annular dark-field scanning transmission electron microscopy (HAADF-STEM). SE-SEM and HAADF-STEM images indicated that the outermost layer of the structure was formed of Au-15 NPs, with the Au-30 NPs selectively located inside (Figures 2d and S3). To confirm this size segregation phenomenon, mixtures of Au-30 and Au-5 NPs ($N_{Au\text{-}5}$:$N_{Au\text{-}30}$ = 100:1) or Au-30 and Au-10 NPs ($N_{Au\text{-}10}$:$N_{Au\text{-}30}$ = 10:1) were also examined. In both cases, SE-SEM images showed that the Au-5 or Au-10 NPs formed a single surface layer (Figures 2b,c, S4, and S5), with HAADF-STEM images showing the Au-30 NPs located inside the assemblies (Figures 2e,f, S4, and S5). There was no obvious difference in size between assemblies with different NP pairs in Figure 2. The size-limiting behavior might be involved to determine the size of these assemblies.[35] When using Au-5 or Au-10 as the smaller NPs, the encapsulated Au-30 NPs can be seen through the outer layer, even in SE-SEM images. The interparticle gap for small GNPs was clearly wider than that for the vesicle structures produced by small GNPs alone (Figure S10), which is probably due to the osmotic pressure. To confirm generality of size-segregated behaviors, we used Au-15 NPs as large particles, which produced vesicle structures (Figure 1). The binary mixture of GFL-Au-5/Au-15 ($N_{Au\text{-}5}$:$N_{Au\text{-}15}$ = 25:1) also showed size segregation (Figure S7). This indicates that the size segregation phenomenon in this study is related to vesicle formation of the small NPs, but is independent of whether the large NPs alone form vesicles.

STEM tomographic slice sections of the segregation of small (5 nm) and large (30 nm) NPs demonstrated that the assemblies are yolk/shell structure, in which a space exists between the interior assembly of Au-30 NPs and outermost layer assembly of Au-5 NPs (Figure 3a,b).[36,37] Figure 3c

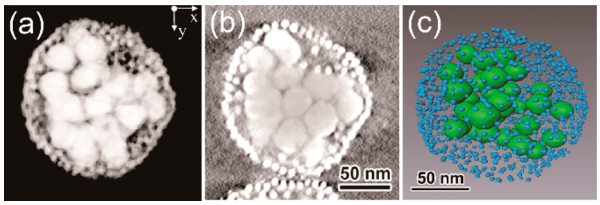

Figure 3. (a) 3D reconstructed image of a GFL-Au-5/Au-30 assembly. Due to the insufficient tilt angular range in TEMT experiments, the 3D image appeared vague, especially in the Z direction. (b) Digitally sliced XY image from 3D reconstructed data. The Z position of the sliced image corresponds to the middle of the GFL-Au-5/Au-30 assembly. (c) Schematic 3D representation of the GFL-Au-5/Au-30 assembly. The center coordinates of all gold nanoparticles (both 5 and 30 nm particles) were determined from the experimentally obtained reconstructed 3D image (a), and virtual particles were generated from the center coordinates. The 3D picture captures the structural features but is not quantitative.

indicates a schematic presentation of Au-5 and Au-30 assembly obtained from TEMT, in which NP shapes were subjected to the spherical approximation. Sliced images of Figure 3c also clearly support the yolk/shell structure (Figure S6).

When the proportionality of the small NPs (Au-5, -10, and -15 NPs) was reduced to $N_{small\text{-}NP}$:$N_{Au\text{-}30}$ = 1:1, no obvious size segregation was observed (Figure S7). At this ratio, the total number of small NPs was insufficient to form Au-30-encapsulated size-segregated structures. In other words, the large excess number of small particles is required for the size segregation, supporting that the small GNPs formed vesicles by pushing large particles into the inner space due to entropy-driven depletion force.[38]

To understand the dynamic size segregation phenomenon, a time-dependent study of the self-assembly of Au-30 and Au-15 NPs ($N_{Au\text{-}15}$:$N_{Au\text{-}30}$ = 7:1) with GFL was carried out (Figures 4 and S8). Samples (3 μL) of the mixture were taken at the times shown in Figure 4, cast onto the TEM grid, and were subjected to drying. STEM images taken soon after mixing showed that

DOI: 10.1021/jacs.5b12456
J. Am. Chem. Soc. 2016, 138, 3274–3277

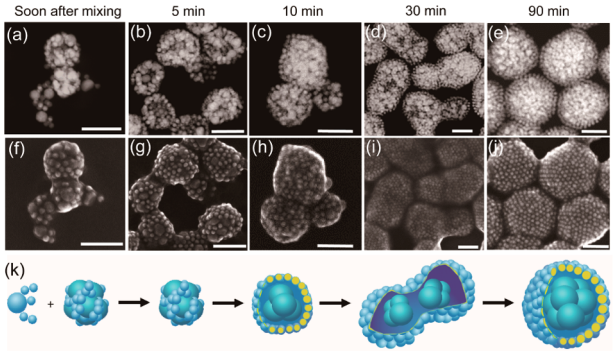

Figure 4. Time-course study of the self-assembly of a mixture of Au-15 and Au-30 in the presence of GFLs. Time dependence on (a–e) HAADF-STEM and (f–j) SE-SEM images of the assemblies at different time points. All scale bars are 100 nm. (k) Scheme of the proposed self-assembly process of a size-segregated yolk/shell assembly.

the Au-30 and Au-15 NPs had already started to form small aggregations. After 5 min, the Au-15 NPs had started to form vesicles with the Au-30 NPs located inside, supporting the notion that the size segregation occurred at the early stage of assembly process. The aggregations were fused into size-segregated assemblies (5–30 min) and grown to spherical assemblies so that the surfaces were covered by Au-15 NPs, while the Au-30 NP assemblies were encapsulated. The image taken after 30 min clearly indicates that the yolk/shell structure was formed via a fusion of the outer layer of each assembly, similar in manner to the fusion of liposomes.

We investigated the ligand exchange rate of GFLs for Au-15 or Au-30 NPs using inductively coupled plasma optical emission spectroscopy (ICP-OES). GFL density on the surface of Au-15 or Au-30 NPs at 5 and 90 min remained almost constant, indicating that the ligand exchange for Au-15 or Au-30 NPs was completed within 5 min (Table S3), while the size segregation took more than 90 min. Importantly, tetra(ethylene glycol)-terminated fluorinated OEG ligands, which lack a glucose moiety, induced aggregations but not size-segregated structures (Figure S9). In some previous literature on supraparticle assemblies, surface ligands have been used as a stabilizer.[39,40] GFL is a unique molecule that affords surface characteristics that enable the rearrangement of GNPs after initial aggregation, resulting in a thermodynamically stable yolk/shell structure. These data suggest that the fluorinated GFL surface promotes the rearrangement of GNPs after initial aggregation in solution, resulting in a thermodynamically stable yolk/shell structure. A time-course study using DLS measurements and UV–vis spectroscopy of these processes suggest that the self-assembly process took place in solution (Figure S11).

All electron microscopy measurements in this study were, however, made for dried samples dispersed on substrates in vacuum. To discuss a formation of hierarchical self-assembly, it is necessary to prove that the yolk/shell assembly is spontaneously formed in solution, but not during the drying process. Pulsed coherent X-ray solution scattering (PCXSS) utilizing X-ray free electron laser, which has been proved as a powerful method to capture snapshots of substances "in solution", such as NP assemblies[41] and living bacteria,[42] was applied to disclose whether or not the assemblies are truly formed in solution.

The image reconstructed from a single-shot coherent X-ray diffraction (CXD) pattern of an isolated assembly indicates the two-dimensional projection of electron density distribution (Figure 5). PCXSS snapshots were captured after the

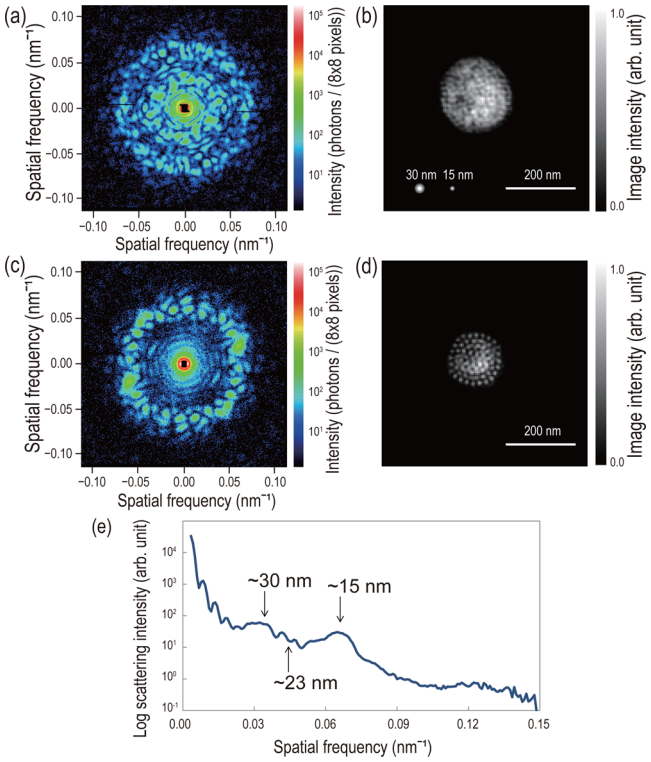

Figure 5. Experimental coherent X-ray diffraction pattern (a,c) and reconstructed image (b,d) of GFL-Au-15/Au-30 NP assembly (a,b) and GFL-Au-15 NP assembly (c,d) in water-containing dioxane solution, measured by single-shot illumination by a femtosecond X-ray laser pulse. (e) Circular average of the CXD pattern of (a).

incubation of GFL with homogeneous mixture of Au-15 and Au-30 NPs for 3 h. Based on Figure 4, 3 h is long enough for the formation of the yolk/shell structure. The diameters of reconstructed image for Au-15/Au-30 mixture and Au-15 alone were approximately 200 and 150 nm, respectively, which were close to the average size obtained from electron microscopy and DLS measurement. The reconstructed images of the binary mixture of Au-15/Au-30 showed yolk/shell structure where Au-15 NPs form the outermost layer with Au-30 NPs located inside, while the images of the assembly made of Au-15 alone showed vesicles with a single layer. Figure 5e shows a circular average of the CXD pattern of Figure 5a. The circular average of the CXD pattern from the binary mixture of Au-15/Au-30 displays that the peaks due to structures with 15 nm periodicity, neighboring Au-15 particles, and 30 nm periodicity, neighboring Au-30 particles, were stronger than that with 23 nm periodicity, neighboring Au-15 and Au-30 particles. This also strongly supports the segregation state of the binary mixture of Au-15 and Au-30 NPs in solution.

In summary, we have demonstrated that binary mixtures of GNPs coated with GFL could hierarchically assemble into a yolk/shell structure in solution. Time-course studies revealed that the size segregation occurred at the early stage of the self-assembly. The kinetically trapped aggregations transformed to energetically stable size-segregated yolk/shell structures. A snapshot obtained by PCXSS clearly indicates that the size-segregated assembly was formed in solution. Our data indicate that the entropy-driven size segregation of fluorinated nano-

DOI: 10.1021/jacs.5b12456
J. Am. Chem. Soc. 2016, 138, 3274–3277

particles is powerful to make hierarchical assembly and this strategy has potential applications to the construction of new types of assembled structures with variable properties.

■ ASSOCIATED CONTENT

Supporting Information

The Supporting Information is available free of charge on the ACS Publications website at DOI: 10.1021/jacs.5b12456.

Experimental details, including Scheme S1, Tables S1−S3, and Figures S1−S17 (PDF)

Supporting Movie 1, demonstrating a spherical hollow structure with a monolayer of GNPs (AVI)

■ AUTHOR INFORMATION

Corresponding Authors

*kniikura@poly.es.hokudai.ac.jp

*hjinnai@tagen.tohoku.ac.jp

*yoshinori.nishino@es.hokudai.ac.jp

Author Contributions

¶J.W. and K.N. contributed equally.

Notes

The authors declare no competing financial interest.

■ ACKNOWLEDGMENTS

This work was supported by JSPS KAKENHI 25286001 and 15H05737; the X-ray Free Electron Laser Priority Strategy Program from the Ministry of Education, Sports, Culture, Science and Technology, Japan (MEXT); CREST from the Japan Science and Technology Agency (JST); and the Cooperative Research Program of "Nano-Macro Materials, Devices and System Research Alliance". J.W. thanks Dr. H. Yabu, Mr. Y. Hirai, and other members in Prof. Jinnai's laboratory for their help with the electron tomography. The XFEL experiments were performed at the BL3 of SACLA with the approval of the Japan Synchrotron Radiation Research Institute (JASRI) (Proposal Nos. 2015A8052, 2014B8053, and 2014A8035). We thank the operation and engineering staff of SACLA for helping perform the PCXSS experiment, and Ms. M. Kuramoto and Mr. M. Takei for fabricating the sample holder. A part of this work was conducted at Hokkaido University, supported by "Nanotechnology Platform" Program of MEXT, Japan.

■ REFERENCES

(1) Nie, Z.; Petukhova, A.; Kumacheva, E. *Nat. Nanotechnol.* **2010**, *5*, 15.

(2) Okamoto, K.; Lin, B.; Imazu, K.; Yoshida, A.; Toma, K.; Toma, M.; Tamada, K. *Plasmonics* **2013**, *8*, 581.

(3) Mohanan, J. L.; Arachchige, I. U.; Brock, S. L. *Science* **2005**, *307*, 397.

(4) Teranishi, T.; Hasegawa, S.; Shimizu, T.; Miyake, M. *Adv. Mater.* **2001**, *13*, 1699.

(5) Guo, S.; Sun, S. *J. Am. Chem. Soc.* **2012**, *134*, 2492.

(6) Boles, M. A.; Talapin, D. V. *J. Am. Chem. Soc.* **2015**, *137*, 4494.

(7) Macfarlane, R. J.; Lee, B.; Jones, M. R.; Harris, N.; Schatz, G. C.; Mirkin, C. A. *Science* **2011**, *334*, 204.

(8) Jones, M. R.; Osberg, K. D.; Macfarlane, R. J.; Langille, M. R.; Mirkin, C. A. *Chem. Rev.* **2011**, *111*, 3736.

(9) Wilner, O. I.; Willner, I. *Chem. Rev.* **2012**, *112*, 2528.

(10) Nealon, G. L.; Greget, R.; Dominguez, C.; Nagy, Z. T.; Guillon, D.; Gallani, J.-L.; Donnio, B. *Beilstein J. Org. Chem.* **2012**, *8*, 349.

(11) Saliba, S.; Mingotaud, C.; Kahn, M. L.; Marty, J.-D. *Nanoscale* **2013**, *5*, 6641.

(12) Lewandowski, W.; Wójcik, M.; Górecka, E. *ChemPhysChem* **2014**, *15*, 1283.

(13) Srivastava, S.; Frankamp, B. L.; Rotello, V. M. *Chem. Mater.* **2005**, *17*, 487.

(14) Donnio, B.; García-Vázquez, P.; Gallani, J. L.; Guillon, D.; Terazzi, E. *Adv. Mater.* **2007**, *19*, 3534.

(15) Kanie, K.; Matsubara, M.; Zeng, X.; Liu, F.; Ungar, G.; Nakamura, H.; Muramatsu, A. *J. Am. Chem. Soc.* **2012**, *134*, 808.

(16) Jishkariani, D.; Diroll, B. T.; Cargnello, M.; Klein, D. R.; Hough, L. A.; Murray, C. B.; Donnio, B. *J. Am. Chem. Soc.* **2015**, *137*, 10728.

(17) Evers, W. H.; Nijs, B. D.; Filion, L.; Castillo, S.; Dijkstra, M.; Vanmaekelbergh, D. *Nano Lett.* **2010**, *10*, 4235.

(18) Talapin, D. V.; Shevchenko, E. V.; Bodnarchuk, M. I.; Ye, X.; Chen, J.; Murray, C. B. *Nature* **2009**, *461*, 964.

(19) Shevchenko, E. V.; Talapin, D. V.; Kotov, N. A.; O'Brien, S.; Murray, C. B. *Nature* **2006**, *439*, 55.

(20) Redl, F. X.; Cho, K. S.; Murray, C. B.; O'Brien, S. *Nature* **2003**, *423*, 968.

(21) Sau, T. K.; Murphy, C. J. *Langmuir* **2005**, *21*, 2923.

(22) Ben-Simon, A.; Eshet, H.; Rabani, E. *ACS Nano* **2013**, *7*, 978.

(23) Yamaki, M.; Higo, J.; Nagayama, K. *Langmuir* **1995**, *11*, 2975.

(24) Kiely, C. J.; Fink, J.; Brust, M.; Bethell, D.; Schiffrin, D. J. *Nature* **1998**, *396*, 444.

(25) Liu, Y.; Liu, Y.; Tao, P.; Shang, W.; Song, C.; Deng, T. *Nanoscale* **2014**, *6*, 14662.

(26) Zellmer, S.; Garnweitner, G.; Breinlinger, T.; Kraft, T.; Schilde, C. *ACS Nano* **2015**, *9*, 10749.

(27) Bishop, K. J.; Wilmer, C. E.; Soh, S.; Grzybowski, B. A. *Small* **2009**, *5*, 1600.

(28) Glotzer, S. C. *Chem. Eng. Sci.* **2015**, *121*, 3.

(29) Li, F.; Josephson, D. P.; Stein, A. *Angew. Chem., Int. Ed.* **2011**, *50*, 360.

(30) Niikura, K.; Iyo, N.; Higuchi, T.; Nishio, T.; Jinnai, H.; Fujitani, N.; Ijiro, K. *J. Am. Chem. Soc.* **2012**, *134*, 7632.

(31) He, J.; Liu, Y.; Babu, T.; Wei, Z.; Nie, Z. *J. Am. Chem. Soc.* **2012**, *134*, 11342.

(32) Song, J.; Cheng, L.; Liu, A.; Yin, J.; Kuang, M.; Duan, H. *J. Am. Chem. Soc.* **2011**, *133*, 10760.

(33) Carcabal, P.; Jockusch, R. A.; Hunig, I.; Snoek, L. C.; Kroemer, R. T.; Davis, B. G.; Gamblin, D. P.; Compagnon, I.; Oomens, J.; Simons, J. P. *J. Am. Chem. Soc.* **2005**, *127*, 11414.

(34) Lopez de la Paz, M.; Ellis, G.; Perez, M.; Perkins, J.; Jimenez-Barbero, J.; Vicent, C. *Eur. J. Org. Chem.* **2002**, *2002*, 840.

(35) Xia, Y.; Nguyen, T. D.; Yang, M.; Lee, B.; Santos, A.; Podsiadlo, P.; Tang, Z.; Glotzer, S. C.; Kotov, N. A. *Nat. Nanotechnol.* **2011**, *6*, 580.

(36) Jinnai, H.; Spontak, R. J.; Nishi, T. *Macromolecules* **2010**, *43*, 1675.

(37) Motoki, S.; Kaneko, T.; Aoyama, Y.; Nishioka, H.; Okura, Y.; Kondo, Y.; Jinnai, H. *J. Electron Microsc.* **2010**, *59*, S45.

(38) Frenkel, D. *Nat. Mater.* **2015**, *14*, 9.

(39) Chen, O.; Riedemann, L.; Etoc, F.; Herrmann, H.; Coppey, M.; Barch, M.; Farrar, C. T.; Zhao, J.; Bruns, O. T.; Wei, H.; Guo, P.; Cui, J.; Jensen, R.; Chen, Y.; Harris, D. K.; Cordero, J. M.; Wang, Z.; Jasanoff, A.; Fukumura, D.; Reimer, R.; Dahan, M.; Jain, R. K.; Bawendi, M. G. *Nat. Commun.* **2014**, *5*, 5093.

(40) de Nijs, B.; Dussi, S.; Smallenburg, F.; Meeldijk, J. D.; Groenendijk, D. J.; Filion, L.; Imhof, A.; van Blaaderen, A.; Dijkstra, M. *Nat. Mater.* **2015**, *14*, 56.

(41) Iida, R.; Kawamura, H.; Niikura, K.; Kimura, T.; Sekiguchi, S.; Joti, Y.; Bessho, Y.; Mitomo, H.; Nishino, Y.; Ijiro, K. *Langmuir* **2015**, *31*, 4054.

(42) Kimura, T.; Joti, Y.; Shibuya, A.; Song, C.; Kim, S.; Tono, K.; Yabashi, M.; Tamakoshi, M.; Moriya, T.; Oshima, T.; Ishikawa, T.; Bessho, Y.; Nishino, Y. *Nat. Commun.* **2014**, *5*, 3052.

DOI: 10.1021/jacs.5b12456
J. Am. Chem. Soc. 2016, 138, 3274−3277